

# Accurate respiratory sound classification model based on piccolo pattern

Beyda Tasar<sup>a</sup>, Orhan Yaman<sup>b,\*</sup>, Turker Tuncer<sup>b</sup>

<sup>a</sup> Department of Mechatronics Engineering, Engineering Faculty, Firat University, Elazig, Turkey

<sup>b</sup> Department of Digital Forensics Engineering, Technology Faculty, Firat University, Elazig, Turkey

## ARTICLE INFO

### Article history:

Received 16 April 2021

Received in revised form 23 November 2021

Accepted 9 December 2021

Available online 18 December 2021

### Keywords:

Pulmonary diseases

Lung sound analysis

Piccolo pattern

NCA feature selection

TQWT

## ABSTRACT

Auscultation, or listening to body sounds with a stethoscope, is the most basic and instructive part of the physical examination. Although it is a quick and effective way of diagnosing respiratory tract disorders, the precision of the diagnosis demands a considerable deal of clinical knowledge. As a result, we've created a computerized diagnostic system that will detect breathing sounds automatically, assisting physicians and trainees in the specialization process. Automated respiratory sound classification is a complex issue for advanced biomedical signal processing. Therefore, variable models and methods have been introduced to overcome this problem. This research aims to introduce a high accurate sound classification model using a nonlinear histogram-based generator. To reach this aim, piccolo pattern (it uses S-box of the piccolo cipher as a pattern), statistical moments, tunable q-factor wavelet transform (TQWT), iterative neighborhood component analysis (INCA), and conventional classifiers are used together. This model uses TQWT to create levels. Piccolo pattern is employed to generate textural features (it is the main feature generator of this model), and statistics are deployed to extract statistical features. INCA chooses the relevant features. Decision tree (DT), support vector machine (SVM), and k nearest neighbors (KNN) classifiers are applied to the selected feature vectors to calculate results. Three cases are defined using ICHBI 2017 dataset to calculate results comprehensively. The defined cases contain seven, three, and eight categories, respectively.

Furthermore, five performance calculation metrics are employed to evaluate the presented piccolo-pattern-based model comprehensively. The introduced piccolo pattern-based model reaches 99.45%, 99.31%, and 99.19% accuracies for Case 1, Case 2, and Case 3 by employing KNN. These accuracies denote the success of the piccolo pattern-based model. Furthermore, this model attains higher accuracies than the previously presented deep learning-based methods for respiratory sound classification.

© 2021 Published by Elsevier Ltd.

## 1. Introduction

### 1.1. Background

The lungs are exposed to smoke, all kinds of particles, chemicals, viruses, and living organisms in the air at any time. In other words, the lungs are open and vulnerable to infections and injuries from the external environment [1]. Respiratory diseases are increasing day by day due to insufficient ventilation, toxic smoke from biomass burning, smoking, etc. Respiratory diseases have the second-highest mortality rate after chronic heart diseases [2]. And it poses a high health burden cost worldwide. The most severe lung diseases and the highest mortality rates are COPD, asthma, and lower respiratory tract infections [1]. According to the latest report of the World Health Organization, 65 million people have

the severe chronic obstructive pulmonary disease (COPD), and about 3 million people die from this disease each year [3,4]. Worldwide, 334 million people suffer from asthma [5,6]. Acute lower respiratory tract infections are among the top three causes of death and disability in both children and adults. Respiratory infections caused by influenza kill 250,000 to 500,000 people each year and cost between \$71 and \$167 billion annually [7]. In the epidemic in 2015, 10.4 million people developed tuberculosis (TB), and 1.4 million died from it [8]. Every year, an average of 1.6 million people die from lung cancer, which kills every year [9] and this rate is increasing every year.

That is one of the most common causes of increased mortality in the world is respiratory diseases [10]. Respiratory sounds are the simplest data used for the detection of respiratory diseases. Respiratory sounds are indicators of air movement, changes in lung tissue, and the location of secretions in the tracheobronchial tree, such as respiratory health and respiratory conditions. Recognition and operation of respiratory sound are important components of

\* Corresponding author.

E-mail address: [orhanyaman@firat.edu.tr](mailto:orhanyaman@firat.edu.tr) (O. Yaman).

pulmonary pathology [11,12]. Many respiratory diseases cause differentiation in the sound generated during respiration. Such illnesses as Asthma, COPD (Chronic Obstructive Pulmonary Disease), pneumonia can be distinguished from differences and abnormalities in breathing sound. In an obstructed or restricted respiratory system, the sound of breathing decreases, or unusual rhythms and noises are added to the normal respiratory sound. Experts perform auscultation using a stethoscope to detect abnormalities in breathing sounds in patients and use this information to make a diagnosis [13]. Auscultation is a simple, non-invasive, harmless, and rapid method used by physicians to classify patients with pulmonary disease using a stethoscope [14,15].

Breathing sounds are generally divided into two classes as normal or abnormal breathing sounds. Normal sound is low noise at a seldom noticeable volume. On the other hand, abnormal sounds can be both continuous and irregular sounds, similar to a regular and continuous high-frequency wheezing, or irregular and brief resembling a crackling or squeaking [16]. Depending on the type of lung disease, one or more of these abnormal sounds may occur in an individual's respiratory sound [17].

During the examination, the doctor, listening to the patient's respiratory sound with a stethoscope, can detect and interpret these abnormal sounds, depending on the doctor's level of expertise and knowledge. The most common noises are crackles, wheezes, and rhonchi, and hearing those sounds substantially aids in the diagnosis of pulmonary disorders [17,18]. For example, wheezing is a common clinical sign in patients with obstructive airway conditions such as Asthma and COPD [19]. Wheezing is a melodic high-pitched sound that is linked to respiratory illnesses including asthma and chronic obstructive pulmonary disease (COPD). Typically, wheezing is found in asthma and chronic obstructive lung diseases. Wheezes can be so loud you can hear them just by standing next to the patient. Patients with parenchymal lung illnesses such as pneumonia experience brief, abrupt, and non-musical crackles [19–21]. Rhonchi are melodious low-pitched sounds that sound similar to snoring and are mainly caused by air-

way secretions that are cleansed by coughing [20]. Crackles, on the other hand, are only heard using a stethoscope, and they are a sign of too much fluid in the lung. Crackles and wheezes are indications of the pathology [22].

## 1.2. Literature review

Table 1 lists studies on automatic respiratory sound classification using ICBHI/ICBHI 17 datasets. The selected state-of-art researches are given in Table 1.

Shovo et al. [31] proposed a mild convolutional neural network (CNN) architecture to classify respiratory diseases from respiratory sound using hybrid scalogram-based features of lung sounds. They trained and tested the success of CNN networks using the ICBHI 2017 lung sound dataset. They declared that the method they proposed had a success of 98.92% chronic classification in three classes and 98.70% in classification with six classes. Jaber et al. [14] proposed a method to estimate six types of respiratory pathologies. According to the experimental results, Improved Random, Gradient Boosting, and AdaBoost classification accuracy was 98.76%, 96.29%, 94.71%, respectively. Naqvi et al. [33] conducted research on the diagnosis of COPD and pneumonia diseases from respiratory noise. While creating the ICBHI dataset, they used the left sound data of normal, pneumonia, and COPD patients taken from Meditron, Littmann 3200, and Littmann Classic stethoscopes as recording devices [33]. Fraiwan et al. [36] investigated the application of different homogeneous collective learning methods for the detection of respiratory diseases. They used decision tree, linear discriminant, support vector machine, and closest neighbor algorithms as classifiers and achieved average classification accuracy as 93.40%, 86.41%, 98.2%, and 97.04%, respectively. Mukherjee et al. [37] used the Linear Predictive Cepstral Coefficient (LPCC) based feature extraction and the Multilayer Perceptron (MLP) based classifier to detect respiratory sounds from patients with respiratory tract infections. With the method they developed, they managed to classify respiratory sounds in the ICBHI17 dataset as normal or

**Table 1**  
Summary of studies conducted on pulmonary diseases classification.

| References and year          | Datasets | Number of Classes | Methods                                  | Results (%)   |
|------------------------------|----------|-------------------|--|---|
| Jaber et al.[14], 2020       | –        | 7                 | Improved-RF, Gradient Boosting, AdaBoost | Acc = 98.76, Pre = 99.23, Rec = 98.4, F-Sc = 98.89  |
| Shuvo et al.[31], 2020       | ICBHI 17 | 3                 | Lightweight CNN                          | Acc = 98.9, Pre = 100, Rec = 98.9, F-Sc = 99.4      |
|                              |          | 6                 |  | Acc = 98.7, Pre = 100, Rec = 98.6, F-Sc = 99.3      |
| Yang et al.[32], 2020        | ICBHI 17 | 4                 | bi-ResNet                                | Acc = 50.16, Pre = 31.12, Rec = 69.2                |
| Naqvi et al.[33], 2020       | ICBHI    | 3                 | DT, LD, SVM                              | Acc = 97.7  |
| Ntalampiras et al.[34], 2020 | ICBHI    | 4                 | DAG-HMM                                  | Acc = 50.1  |
| Minami et al.[35], 2019      | ICBHI    | 4                 | CNN                                      | Acc = 50, Pre = 69, Rec = 36                        |
| Fraiwan et al.[36], 2021     | ICBHI    | 6                 | Boosted DT                               | Acc = 98.27, F-Sc = 93.61                           |
| Mukhe et al.[37], 2021       | ICBHI 17 | 2                 | Multilayer Perceptron                    | Acc = 99.2  |
| Li et al.[38], 2020          | ICBHI    | 5                 | CNN attention                            | Acc = 67  |
| Demir et al.[39], 2020       | ICBHI 17 | 4                 | LDA /RSE                                 | Acc = 71.15, Pre = 86, Rec = 61, F-Sc = 65          |
| Pham et al.[40], 2020        | ICBHI 17 | 4                 | CNN                                      | Acc = 79, Pre = 90, Rec = 68                        |
|                              |          | 2                 |  | Acc = 84, Pre = 90, Rec = 78                        |
| Demir et al.[41], 2020       | ICBHI 17 | 4                 | SVM                                      | Acc = 68.5, Pre = 83, Rec = 53, F-Sc = 55           |
| Nguyen et al.[42], 2020      | ICBHI 17 | 4                 | CNN                                      | Pre = 85.32, Rec = 84.11, F-Sc = 84.71              |
| Ngo et al.[43], 2020         | ICBHI    | 4                 | CNN + Autoencoder                        | Acc = 49, Pre = 69, Rec = 30                        |
| Acharya et al.[44], 2020     | ICBHI 17 | 4                 | Hybrid CNN + RNN                         | Acc = 71.81, Pre = 86.7, Rec = 56.91                |
| Hazra et al.[45], 2020       | ICBHI    | 6                 | 2D CNN                                   | Acc = 92, Pre = 71.83, Rec = 50.83, F-Sc = 54.83    |
| Pham et al.[46,47], 2020     | ICBHI    | 4                 | Inception NN                             | Acc = 86, Pre = 88, Rec = 85                        |
| Nguyen et al.[48], 2020      | ICBHI    | 4                 | CNN                                      | Acc = 78.4, Pre = 87.3, Rec = 69.4                  |
|                              |          | 2                 |  | Acc = 83.7, Pre = 87.3, Rec = 80.01                 |
| Ma et al.[49], 2019          | ICBHI 17 | 4                 | Bi-ResNet                                | Acc = 52.79, Pre = 69.2, Rec = 31.12, F-Sc = 50.16  |
| Paraschiv et al.[50], 2020   | ICBHI 17 | 6                 | MFCC, CNN                                | Acc = 90.21, F-Sc = 89                              |
| Monaco et al.[51], 2020      | ICBHI    | 2                 | DNN                                      | Acc = 82, Pre = 87                                  |
| Basu et al.[52], 2020        | ICBHI 17 | 6                 | CNN                                      | Acc = 95.67, Pre = 95.89, Rec = 95.65, F-Sc = 95.66 |
| Gairola et al.[53], 2020     | ICBHI    | 4                 | ResNet34                                 | Pre = 83.3, Rec = 53.7, F-Sc = 68.5                 |
|                              |          | 2                 |  | Pre = 80.9, Rec = 73.1, F-Sc = 77                   |

\*Acc = Accuracy, Pre = Precision, Rec = Recall or Sensitivity, and F-Sc = F-Score/F1-Score, CNN = Convolutional neural network, MFCC = Mel-frequency cepstral coefficients, DNN = Deep neural network, NN = Neural network, LDA = Linear Discriminant Analysis, RSE = Random Subspace Ensembles, DAG-HMM = Directed acyclic graph.

abnormal with an accuracy of 99.22%. Nguyen et al. [42] proposed a multiple-entry CNN model. Experimental results demonstrated an 84.71% success in detecting crackles in the unexpected lung sound classification.

Datasets ICBHI and ICBHI17 are widely used for respiratory sound classification. Meditron, Littmann 3200, and Littmann stethoscopes were used in these datasets [33]. Generally, methods have been developed for two, three, four, five, six, and seven classes [33,37,40,45]. In the literature, deep learning-based methods have been developed to classify respiratory sounds. High accuracy was computed with these methods. However, these methods have high computational complexity [40,42,48]. In our method, a lightweight method has developed and higher accuracy than the literature has been calculated.

### 1.3. Motivation and our method

Although auscultation is a non-invasive, real-time, low-cost, and highly informative physical diagnosis approach, it requires a high level of clinical knowledge for effective diagnosis [20,23,24]. Medical students had a success rate of 60.3 percent, interns 53.4 percent, residents 68.8%, and specialist clinicians 80.1 percent in recognizing abnormal lung sounds, according to Kim et al [23]. This conclusion indicates that developing computerized diagnostic tools is critical to reduce the detection level problem, which fluctuates based on physician clinical expertise, and to speed up physicians' decision-making processes. The vast majority of Artificial Intelligence (AI) based breath sound analysis research focuses on automatic detection of respiratory noise types sensor type and location, and sound analysis techniques. There is a need for computer-assisted software that can accurately assess the type of disease based on aberrant biomedical data [25–27].

The primary motivation for this study is to obtain better classification rates using the ICHBI 17 dataset. Feature extraction, feature selection, and machine learning methods are used to achieve high accuracy. Many deep learning models that classify using the ICHBI 17 dataset have been developed in the literature. However, deep learning models require high-spec computers. In this study,

a lightweight method is presented by preferring machine learning algorithms. A cognitive model has been developed in the proposed method as in deep learning networks to achieve high classification accuracy. This model consists of feature extraction, feature selection, and classification stages. A TQWT [28], Piccolo pattern [29], and statistical-based hybrid model are proposed for feature extraction. Thus, feature extraction has been made from the ICHBI 17 sound data. Neighborhood Component Analysis (NCA) algorithm has been preferred to select the most weighted features. NCA, which is an effective feature selection method, is widely used in the literature [30]. The iterative neighborhood component analysis (INCA) method has been used to select the NCA algorithm's optimum features. DT, SVM, and KNN algorithms have been used for the classification of the optimum features selected. Therefore, a lightweight method is proposed in this study.

This study presents a naïve and basic acoustical sound classification method to detect the type of lung disease. In this study, the

**Table 2**

Datasets used for Case 1, Case 2, and Case3, number of classes, and sample numbers.

| Case   | Meditron | LittC2SE | Litt3200 | Number of Class | Number of samples |
|--------|----------|----------|----------|-----------------|-------------------|
| Case 1 | +        | –        | –        | 7               | 2013              |
| Case 2 | –        | +        | –        | 3               | 1740              |
| Case 3 | +        | +        | +        | 8               | 3827              |

**Table 3**

Classes and number of samples for Case 1, Case 2 and Case 3.

| Class | Name           | Case 1 | Case 2 | Case 3 |
|-------|----------------|--------|--------|--------|
| 1     | URTI           | 458    | –      | 458    |
| 2     | Healthy        | 695    | –      | 695    |
| 3     | COPD           | 200    | 1020   | 1294   |
| 4     | Bronchiectasis | 320    | –      | 320    |
| 5     | Pneumonia      | 40     | 700    | 740    |
| 6     | Bronchiolitis  | 260    | –      | 260    |
| 7     | Asthma         | –      | 20     | 20     |
| 8     | LRTI           | 40     | –      | 40     |

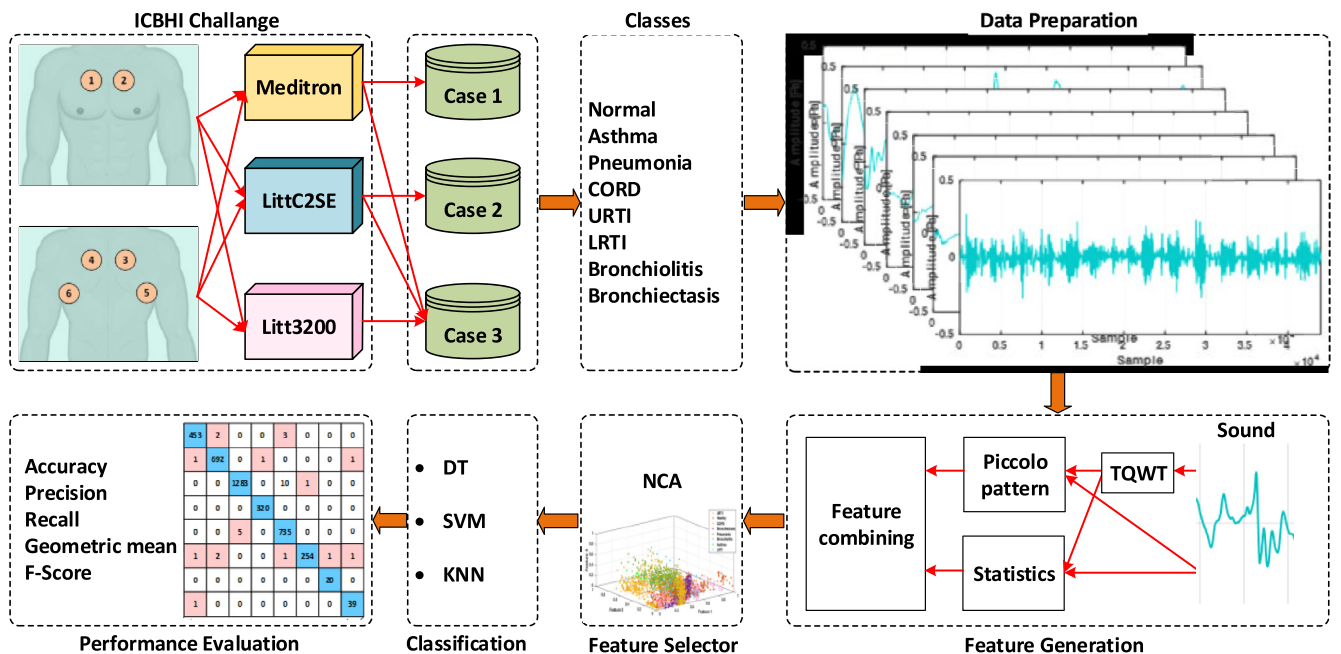


**Fig. 1.** Graphical summarization of the proposed Piccolo Pattern and NCA based lung diagnosis detection.

most reliable and most accessible data type ICHBI17 lung respiratory sound dataset has been used. The graphical summarization of this method is also shown in Fig. 1.

Breathing sounds in this dataset have been collected from 126 individuals for eight different disease types from three different electronic stethoscopes (Meditron-Master Elite Plus Stethoscope,

Littmann 3200, and Littmann Classic). To detect the type of lung disease, a new and naïve method has been presented: Piccolo and INCA-based lung pathology identification method. This method has three fundamental phases: Piccolo-based feature generation, the most meaningful feature selection using INCA, and classification phases.

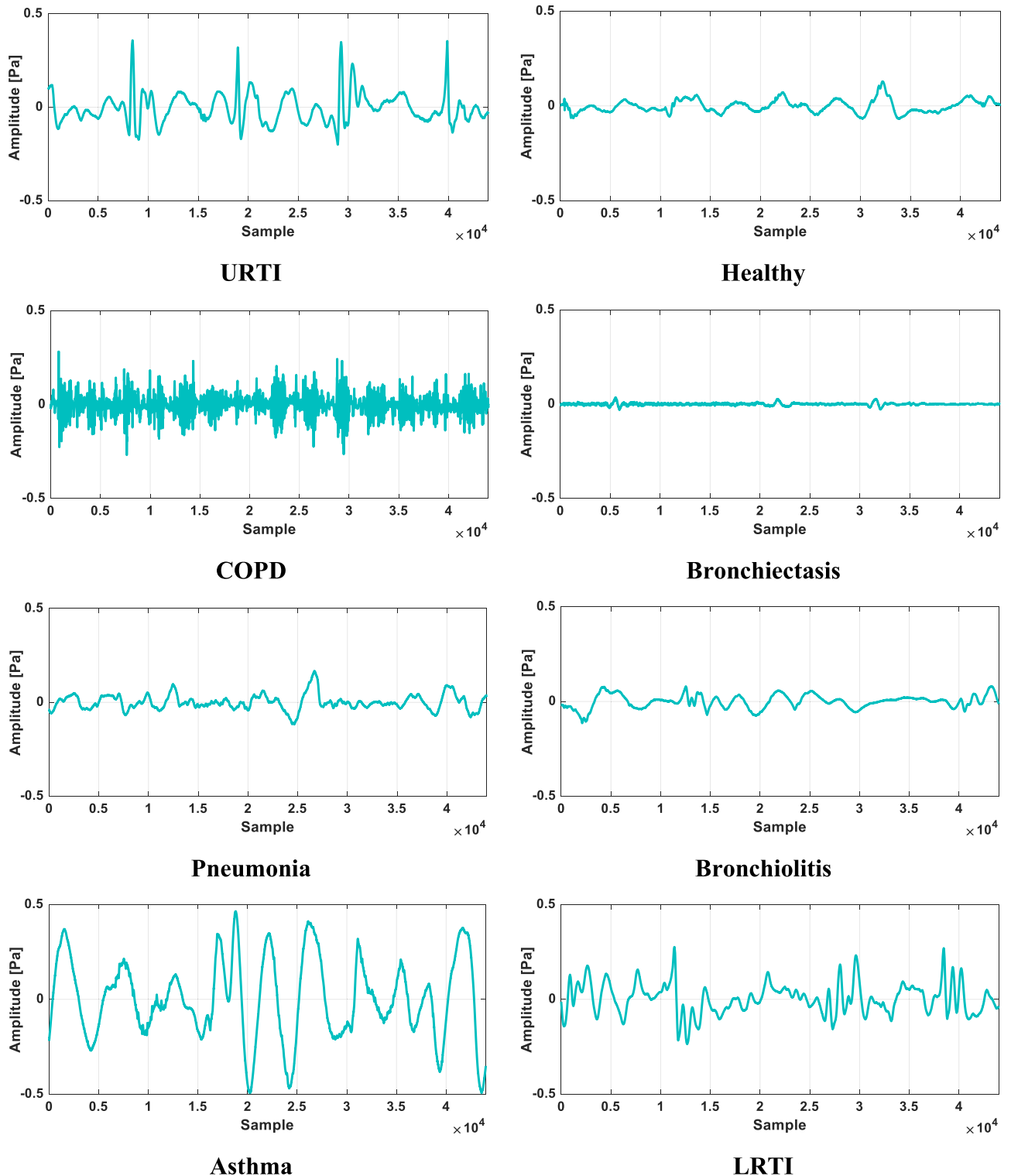
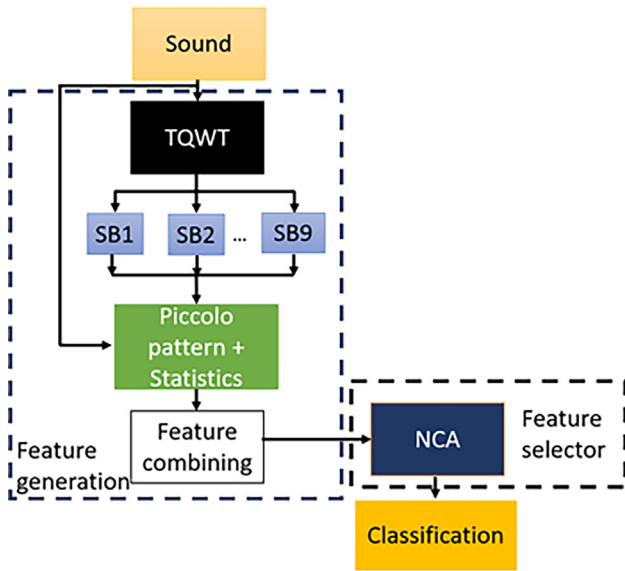


Fig. 2. Sample sound signals for each class.



**Fig. 3.** The schematic denotation of the presented piccolo pattern and INCA-based sound classification model. Herein, SB defines subbands.

**Table 4**  
The presented respiratory sound classification model.

| Input                 | Process   | Output   |
|-----------------------|---|--|
| Sound                 | TQWT ( $Q = 1$ , $r = 2$ , $J = 8$ )                | Nine subbands (SB) with a length of $\{L, \frac{L}{2}, \dots, \frac{L}{256}\}$ , where $L$ is the length of the sound. |
| Sounds and SBs        | Piccolo pattern                                     | $10 \times 512$ sized feature vector   |
| Sounds and SBs        | Piccolo pattern                                     | $10 \times 30$ sized feature vectors   |
| Feature vector        | Feature merging                                     | 5420 sized final feature vector  |
| Merged feature vector | INCA (feature selection)                            | Chosen feature vector with a length of $k$ .   |
| Selected features     | Classification using three conventional classifiers | Results  |

#### 1.4. Contributions

The contributions of the introduced piccolo pattern and INCA based automated respiratory sound classification/detection model are:

- A new generation nonlinear feature generator is introduced, and this function is named piccolo pattern since utilizes the S-Box of the piccolo cipher as a pattern. This function is a new method of the nonlinear feature generation methodology. Hence, this research contributes to the nonlinear histogram-based feature extraction methodology.
- Respiratory/stethoscopic lung sound classification is a complex/hard issue for machine learning. To overcome this problem and denote the success of the introduced piccolo pattern, the novel classification model is presented by deploying TQWT, piccolo pattern, INCA, and three shallow classifiers, and this model attained high performances and outperformed.
- In this study, a lightweight method has been proposed and high accuracy has been calculated in three datasets.

**Table 5**  
S-Box of the piccolo cipher.

| i    | 1  | 2 | 3  | 4 | 5 | 6 | 7 | 8  | 9 | 10 | 11 | 12 | 13 | 14 | 15 | 16 |
|------|----|---|----|---|---|---|---|----|---|----|----|----|----|----|----|----|
| S(i) | 15 | 5 | 12 | 3 | 4 | 9 | 1 | 10 | 2 | 11 | 8  | 16 | 7  | 13 | 5  | 14 |

**Table 6**  
The used statistical moments for feature extraction.

| No | Moment                        | No | Moment                             |
|----|-------------------------------|----|------------------------------------|
| 1  | max(signal)                   | 16 | max(abs(signal))                   |
| 2  | mean(signal)                  | 17 | mean(abs(signal))                  |
| 3  | median(signal)                | 18 | median(abs(signal))                |
| 4  | var(signal)                   | 19 | var(abs(signal))                   |
| 5  | std(signal)                   | 20 | std(abs(signal))                   |
| 6  | min(signal)                   | 21 | min(abs(signal))                   |
| 7  | max(signal)- min(signal)      | 22 | max(abs(signal))- min(abs(signal)) |
| 8  | rms(signal)                   | 23 | rms(abs(signal))                   |
| 9  | sum(signal.^2)                | 24 | sum(abs(signal).^2)                |
| 10 | wentropy(signal,'shannon')    | 25 | wentropy(abs(signal),'shannon')    |
| 11 | wentropy(signal,'sure',1)     | 26 | wentropy(abs(signal),'sure',1)     |
| 12 | wentropy(signal,'log energy') | 27 | wentropy(abs(signal),'log energy') |
| 13 | kurtosis(signal)              | 28 | kurtosis(abs(signal))              |
| 14 | skewness(signal)              | 29 | skewness(abs(signal))              |
| 15 | mad((signal))                 | 30 | mad(abs(signal))                   |

## 2. Materials and methods

### 2.1. Materials

This research uses the publicly available ICBHI 2017 Respiratory Sound Database [10,12]. This dataset includes sound samples collected independently over several years by two research teams in two different countries. The dataset was recorded using three different electronic stethoscopes (Meditron, LittC2SE, Litt3200). Respiratory cycles were labeled by their specialists by dividing them into eight types of lung conditions (URTI (Upper Respiratory Tract Infection), Healthy, COPD (Chronic Obstructive Pulmonary Disease), Bronchiectasis, Pneumonia, Bronchiolitis, Asthma, LRTI (Lower Respiratory Tract Infection))

In this study, a dataset has been created for three different cases (Case 1, Case 2, Case 3) from the respiratory sounds included in the ICBHI 17 dataset, which have been collected with different stethoscopes for different number of disease types. The recording device for each case, the number of disease classes, and the amount of sample sound recording used are shown in Table 2. Table 3 shows the distribution amount of the records in the data used for each condition. Creating three different case scenarios is that data records of eight different diseases with each recorder have been not included in the dataset. In other words, seven types of disease data have been recorded with the Meditron stethoscope, three types of disease data with the LittC2SE stethoscope, and one type of disease data with the Litt3200 dataset. In Case 3, all the data obtained with these three recorders have been collected and analyzed together, and the method suggested for an eight-class classification problem has been tested.

In Fig. 2, examples of respiratory cycle records recorded for eight types of lung disorders (URTI, healthy, COPD, Bronchiectasis, Pneumonia, Bronchiolitis, Asthma, LRTI) are visualized.

### 2.2. The respiratory sound classification method

This study presents a new piccolo pattern and statistical feature generators based respiratory sound classification model. The primary phases of this method are feature extraction, the feature is chosen, and classification. Two feature generators have been used



in the feature generation phase: presented piccolo pattern (it is a nonlinear histogram-based feature generator) and 30 statistical moments. To extract low-level, mid-level, and high-level features, TQWT has been employed in the respiratory sounds, and subbands have been calculated [54,55]. By using this multileveled and generation network, features of the respiratory sounds have been generated. To choose the most distinctive ones, an iterative NCA selector has been deployed. Three shallow classifiers have been deployed for classification. The block diagram of the presented multileveled piccolo pattern and statistical generator-based model is shown in Fig. 3.

As denoted in Fig. 3, the major novelty of the presented model is the introduced piccolo pattern. Piccolo pattern is a nonlinear histogram-based feature generator and uses S-Box of the piccolo lightweight cipher as a pattern to generate features. The steps of the presented model are given in Table 4.

The main phases of the presented model are explained in subsections.

### 2.2.1. Feature generation

Feature extraction has been the first phase of the presented respiratory sound classification model. A high accurate model should generate discriminative features. To reach this aim, a new feature generation network has been presented using TQWT, the presented piccolo pattern, and statistical features. TQWT is a new generation wavelet transformation, and several mother wavelet filters can be defined using Q-factor (Q), redundancy (r), and a number of levels (J) parameters. Q sets the oscillatory value of the signal. If users prefer to employ non-oscillatory transformation, the Q value is selected as one. The TQWT can be used as a decomposer. Herein, 1, 2, and 8 have been selected as Q, r, and J values/parameters, respectively. Herein, non-oscillatory TQWT have been chosen to decompose signals and we used TQWT similar to the pooling operator in the convolutional neural networks. In this work, we aimed to propose a multilevel feature extractor and our feature extractor has nine levels by using the J value as eight since the best classification accuracy has been calculated using these parameters. By employing TQWT, nine subbands have been calculated [28]. The generated nine subbands using TQWT, and the respiratory sound has been used to generate both textural (piccolo pattern) and statistical features. The used two functions (piccolo pattern and statistical moments) extracted 542 features from each signal. In the last step of this phase, the generated features have been merged, and

5420 features have been obtained. This phase is defined in detail below.

**Step 0:** Read each respiratory sound from the dataset.

**Step 1:** Employ TQWT to sound and calculate SBs.

**Step 2:** Extract textural features using the presented piccolo pattern. Piccolo pattern is defined as below. The main objective of this pattern has been to show the feature generation ability of the piccolo cipher S-Box. This S-Box is the main nonlinear function of this cipher [29]. By employing it, a nonlinear histogram-based textural feature generator has been presented.

**Step 2.1:** Create a pattern using the S-Box of the lightweight piccolo cipher. This S-Box is demonstrated in Table 5.

In Table 5,  $i$  denotes input, and  $S(i)$  shows the output. In Table 5, a nonlinear feature generator is presented. The length of the used S-Box has been 16. Thus, the one-dimensional signal has been divided into 16 sized overlapping blocks and  $i$  and  $S(i)$  values have been compared to generate bits.

**Step 2.2:** Divide block into 16 overlapping sized blocks.

**Step 2.3:** Calculate 16 bits using piccolo S-Box pattern.

$$bit(i) = S(B(i), B(S(i))), i = \{1, 2, \dots, 16\} \quad (1)$$

$$S(B(i), B(S(i))) = \begin{cases} 0, & B(i) - B(S(i)) < 0 \\ 1, & B(i) - B(S(i)) \geq 0 \end{cases} \quad (2)$$

Herein,  $B$  is used 16 sized overlapping block and  $S(.,.)$  defines Signum function.

**Step 2.4:** Create two map signals using the generated 16 bits. The one-dimensional local binary pattern and ternary pattern used 8-bit coded histograms. Thus, the generated 16 bits have been divided into two groups with a length of eight. The mathematical notation of the feature map generation is shown in Equation (3).

$$fm^t(h) = \sum_{i=1}^8 bit((t-1)*8+i)*2^{i-1}, t = \{1, 2\} \quad (3)$$

Herein,  $fm^1$  and  $fm^2$  first and second feature map signals.

**Step 2.5:** Generate histograms of the  $fm^1$  and  $fm^2$  signals.

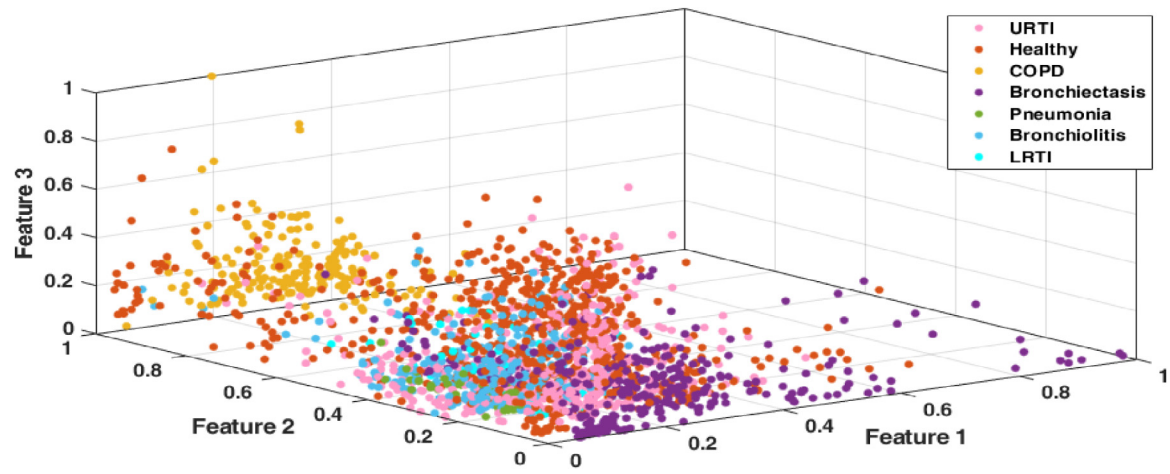
**Step 2.6:** Merge the created histograms and obtain 512 features.

**Step 3:** Generate 30 statistical features from sound and 9 SBs of the used sound. The used 30 statistical moments are given in Table 6.

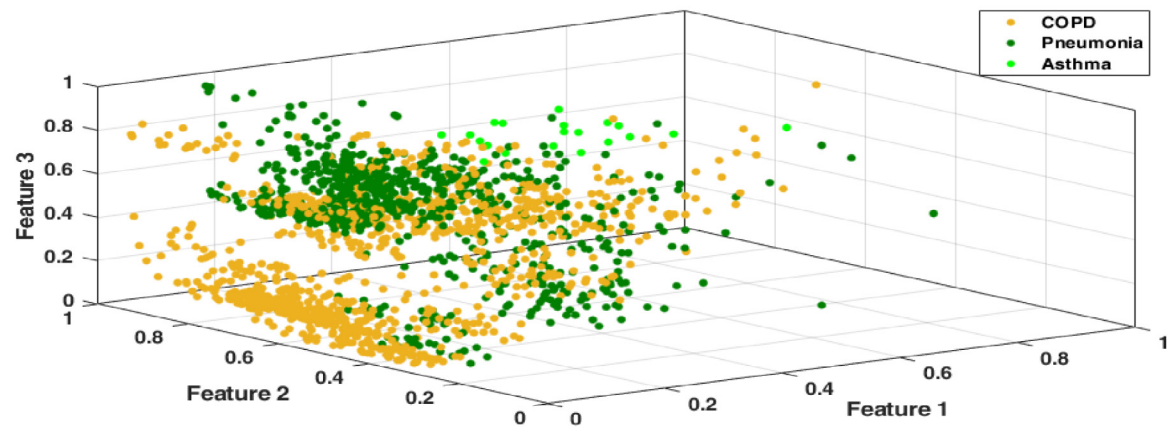
**Step 4:** Fuse the generated all features and extract 5420 features from a sound.

| Procedure: Iterative NCA                        |                         |
|---|-------------------------|
| <b>Input</b>                                    | Load features           |
| <b>Output</b>                                   | Select optimal features |
| 00: Load combined features                      |                         |
| 01: Apply NCA to features and calculate indices |                         |
| 02: <b>for</b> i=LB to UB <b>do</b>             |                         |
| 03:   | Select features         |
| 04:   | Calculate loss value    |
| 05:   | Store loss values       |
| 06: <b>end for i</b>                            |                         |
| 07: Calculate minimum loss value                |                         |
| 08: Select optimal features                     |                         |

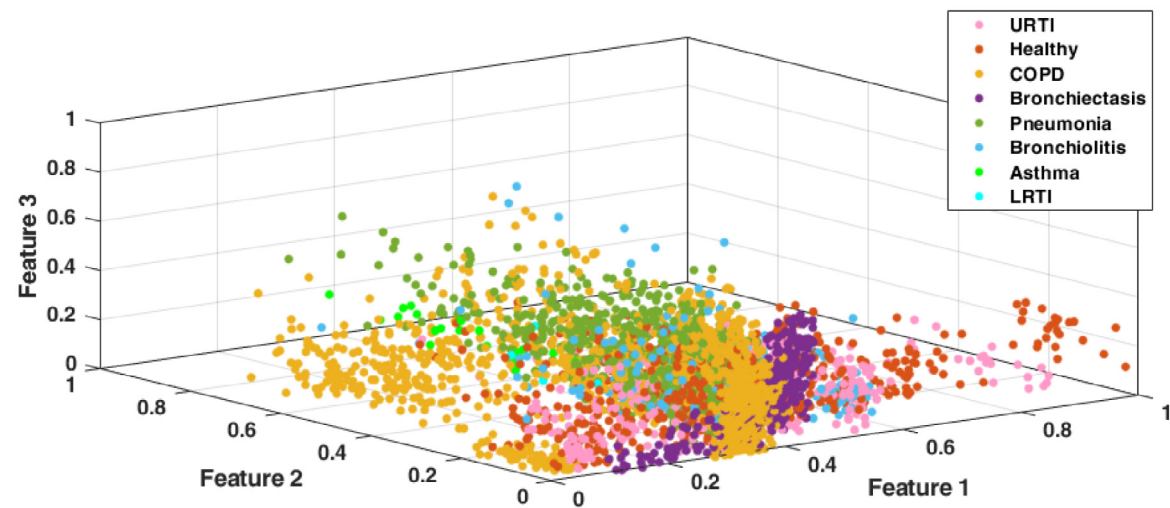
Fig. 4. The pseudocode of the iterative NCA feature selector.



Case 1



Case 2



Case 3

Fig. 5. Scatter plots of selected features in Case1, Case2, and Case3 datasets.

**Table 7**

Parameters of classification algorithms used in the proposed method.

| Parameter                | DT       | SVM        | KNN       |
|--------------------------|----------|------------|-----------|
| Type                     | Fine     | Cubic      | Fine      |
| Split Criterion          | Deviance | –          | –         |
| Maximum Number of Splits | 100      | –          | –         |
| Surrogate                | off      | –          | –         |
| Distance                 | –        | –          | Cityblock |
| Number of Neighbors      | –        | –          | 1         |
| Distance Weight          | –        | –          | Equal     |
| Standardize              | –        | True       | True      |
| Kernel Function          | –        | Polynomial | –         |
| Polynomial Order         | –        | 3          | –         |
| Kernel Scale             | –        | Auto       | –         |
| Box Constraint Level     | –        | 1          | –         |

### 2.2.2. Feature selection

The second phase of the presented piccolo pattern-based sound classification model has been to select the most discriminative features. Therefore, iterative NCA has been used as a feature selector. NCA is a distance-based feature selection method. The NCA algorithm generates positive weights for each feature[56]. Thus, it differs from other feature selection algorithms. NCA algorithm is given in equation (4), and equation (5).

$$P_{ij} = \frac{\exp(-d_{ij})}{Z_{0i}} \quad (4)$$

$$Z_{0i} = \sum_{j \neq i} \exp(-d_{ij}) \quad (5)$$

In Equation 12, the  $i$  value represents the data to be classified, and the  $j$  value refers to neighboring data.  $d_{ij}$  value  $i$ . with data  $j$ . represents the distance between data.

The pseudocode of the Iterative NCA algorithm is shown in Fig. 4.

**Step 5:** Choose the most discriminative features employing INCA to generate 5420 features.

The proposed method has been applied for case1, case 2, and case 3, and the best features have been chosen. For Case 1, feature extraction has been made within the 2013x44100 sample, and 2013x5420 features have been obtained. Later, the 2013x306 feature has been selected with INCA. For Case 2, 1740x5420 features have been obtained by extracting features on 1740x44100 samples. By using the 1740x5420 feature, the 1740x463 feature is selected with iterative INCA. For Case 3, the 3827x451 feature has been selected with iterative INCA on the 3827x44100 sample. Scatter Plot graphs of the features selected in Case1, Case2, and Case3 datasets are shown in Fig. 5.

### 2.2.3. Classification

The classification has been the last phase of the presented model in Table 7. To denote the strength of the presented piccolo pattern-based feature generation and INCA selector, three shallow classifiers have been deployed. 10 fold cross-validation has been used to obtain validation results from these classifiers[57]. To choose classifiers, the MATLAB classification learner tool has been used. The used decision tree classifier is named Fine DT. Fine DT has been used to denote the high classification ability of our extracted features. The used other classifier is a support vector machine and we used a 3rd-degree polynomial kernel. The third classifier is k nearest neighbor. We used 1NN in this work and the distance metric of this classifier is L1-norm (city block/Manhattan). The attributes of the used classifiers are given in below.

**Step 6:** Classify the selected features using DT, SVM or KNN with 10 fold cross-validation.

DT, SVM, and KNN algorithms have been used to classify selected features in the proposed method. DT, SVM, and KNN algorithms have been preferred in this study because they give better accuracy than other traditional algorithms. Traditional classifier results are shown for Case1, Case2, and Case3 in Fig. 6.

As seen in Fig. 6, the accuracy values of DT, Naïve Bayes (NB), Linear Discriminant (LD), SVM, KNN, Ensemble Bagged Tree (EBT), and Ensemble Subspace Discriminant (ESD) algorithms have been calculated. The best results for the seven classification algorithms have been obtained with DT, SVM, and KNN algorithms. Thus DT, SVM, and KNN algorithms have been preferred.

## 3. Performance analysis

### 3.1. Experimental setup

MATLAB2020A and Classification Learner Toolbox have been used in the proposed method. Results have been obtained using a computer with Windows 10 operating system. The recommended method has been implemented on a computer with 256 GB SSD hard disk, 48 GB RAM, intel i7-9700 CPU 3.00 GHz. MATLAB (m) files are used to implement the proposed feature extraction and INCA. To classify the selected features, the Classification Learner Toolbox is used. To achieve the best classification results, we employed the classifiers.

### 3.2. Results

In this study, Case 1, Case 2, and Case 3 have been created using data from Meditron, LittC2SE, Litt3200 devices. Case 1 consisted of seven classes, Case 2 three classes, and Case 3 eight classes. Three classification algorithms have been used to classify these datasets:

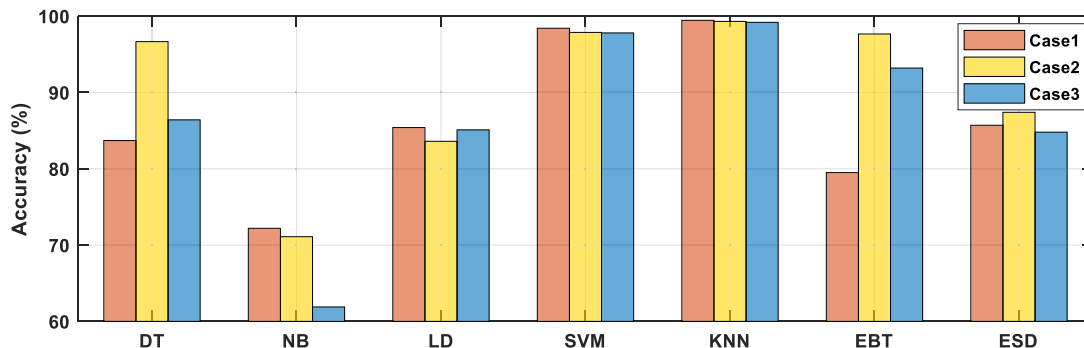


**Fig. 6.** Accuracy results calculated using conventional classifiers for Case 1, Case 2, and Case 3 (10-fold cross-validation).



| True Class | URTI            | 366  | 50      | 0    | 3              | 7         | 27            | 5    |
|------------|-----------------|------|---------|------|----------------|-----------|---------------|------|
|            | Healthy         | 54   | 598     | 1    | 3              | 3         | 33            | 3    |
|            | COPD            | 1    | 2       | 195  | 0              | 0         | 1             | 1    |
|            | Bronchiectasis  | 2    | 3       | 0    | 313            | 0         | 2             | 0    |
|            | Pneumonia       | 7    | 4       | 0    | 0              | 20        | 8             | 1    |
|            | Bronchiolitis   | 31   | 44      | 2    | 2              | 6         | 169           | 6    |
|            | LRTI            | 9    | 3       | 0    | 1              | 2         | 1             | 24   |
|            | Predicted Class | URTI | Healthy | COPD | Bronchiectasis | Pneumonia | Bronchiolitis | LRTI |

DT

| True Class | URTI            | 652  | 5       | 0    | 0              | 0         | 1             | 0    |
|------------|-----------------|------|---------|------|----------------|-----------|---------------|------|
|            | Healthy         | 3    | 690     | 0    | 0              | 0         | 2             | 0    |
|            | COPD            | 0    | 1       | 199  | 0              | 0         | 0             | 0    |
|            | Bronchiectasis  | 0    | 0       | 0    | 320            | 0         | 0             | 0    |
|            | Pneumonia       | 1    | 0       | 0    | 0              | 39        | 0             | 0    |
|            | Bronchiolitis   | 5    | 8       | 0    | 0              | 0         | 246           | 1    |
|            | LRTI            | 4    | 1       | 0    | 0              | 0         | 0             | 35   |
|            | Predicted Class | URTI | Healthy | COPD | Bronchiectasis | Pneumonia | Bronchiolitis | LRTI |

SVM

| True Class | URTI            | 454  | 2       | 0    | 0              | 2         | 0             | 0    |
|------------|-----------------|------|---------|------|----------------|-----------|---------------|------|
|            | Healthy         | 1    | 694     | 0    | 0              | 0         | 0             | 0    |
|            | COPD            | 0    | 0       | 200  | 0              | 0         | 0             | 0    |
|            | Bronchiectasis  | 0    | 0       | 0    | 320            | 0         | 0             | 0    |
|            | Pneumonia       | 0    | 0       | 0    | 0              | 40        | 0             | 0    |
|            | Bronchiolitis   | 1    | 4       | 0    | 0              | 0         | 254           | 1    |
|            | LRTI            | 0    | 0       | 0    | 0              | 0         | 0             | 40   |
|            | Predicted Class | URTI | Healthy | COPD | Bronchiectasis | Pneumonia | Bronchiolitis | LRTI |

KNN

Fig. 7. Confusion matrices for Case1.

| True Class | COPD            | 993  | 26        | 1      |
|------------|-----------------|------|-----------|--------|
|            | Pneumonia       | 21   | 676       | 3      |
|            | Asthma          | 4    | 3         | 13     |
|            | Predicted Class | COPD | Pneumonia | Asthma |

DT

| True Class | COPD            | 999  | 21        | 0      |
|------------|-----------------|------|-----------|--------|
|            | Pneumonia       | 16   | 684       | 0      |
|            | Asthma          | 0    | 0         | 20     |
|            | Predicted Class | COPD | Pneumonia | Asthma |

SVM

| True Class | COPD            | 1010 | 10        | 0      |
|------------|-----------------|------|-----------|--------|
|            | Pneumonia       | 2    | 698       | 0      |
|            | Asthma          | 0    | 0         | 20     |
|            | Predicted Class | COPD | Pneumonia | Asthma |

KNN

Fig. 8. Confusion matrices for Case2.

| True Class      | URTI | Healthy | COPD | Bronchiectasis | Pneumonia | Bronchiolitis | Asthma | LRTI |
|-----------------|------|---------|------|----------------|-----------|---------------|--------|------|
|                 | 346  | 63      | 5    | 0              | 6         | 28            | 0      | 10   |
|                 | 37   | 553     | 11   | 4              | 27        | 29            | 0      | 4    |
|                 | 6    | 16      | 1208 | 4              | 53        | 7             | 0      | 0    |
|                 | 2    | 6       | 3    | 308            | 0         | 1             | 0      | 0    |
|                 | 10   | 11      | 43   | 0              | 660       | 10            | 2      | 4    |
|                 | 20   | 38      | 1    | 0              | 7         | 190           | 0      | 4    |
|                 | 0    | 1       | 2    | 0              | 2         | 0             | 15     | 0    |
|                 | 8    | 2       | 1    | 0              | 1         | 1             | 0      | 27   |
| Predicted Class |      |         |      |                |           |               |        |      |
| DT              |      |         |      |                |           |               |        |      |

| True Class      | URTI | Healthy | COPD | Bronchiectasis | Pneumonia | Bronchiolitis | Asthma | LRTI |
|-----------------|------|---------|------|----------------|-----------|---------------|--------|------|
|                 | 451  | 6       | 0    | 0              | 0         | 1             | 0      | 0    |
|                 | 3    | 689     | 0    | 0              | 1         | 2             | 0      | 0    |
|                 | 1    | 0       | 1261 | 0              | 32        | 0             | 0      | 0    |
|                 | 0    | 0       | 0    | 320            | 0         | 0             | 0      | 0    |
|                 | 2    | 0       | 21   | 0              | 717       | 0             | 0      | 0    |
|                 | 4    | 5       | 0    | 0              | 0         | 250           | 0      | 1    |
|                 | 0    | 0       | 1    | 0              | 0         | 0             | 19     | 0    |
|                 | 2    | 2       | 0    | 0              | 0         | 0             | 0      | 36   |
| Predicted Class |      |         |      |                |           |               |        |      |
| SVM             |      |         |      |                |           |               |        |      |

| True Class      | URTI | Healthy | COPD | Bronchiectasis | Pneumonia | Bronchiolitis | Asthma | LRTI |
|-----------------|------|---------|------|----------------|-----------|---------------|--------|------|
|                 | 453  | 2       | 0    | 0              | 3         | 0             | 0      | 0    |
|                 | 1    | 692     | 0    | 1              | 0         | 0             | 0      | 1    |
|                 | 0    | 0       | 1283 | 0              | 10        | 1             | 0      | 0    |
|                 | 0    | 0       | 0    | 320            | 0         | 0             | 0      | 0    |
|                 | 0    | 0       | 5    | 0              | 735       | 0             | 0      | 0    |
|                 | 1    | 2       | 0    | 0              | 1         | 254           | 1      | 1    |
|                 | 0    | 0       | 0    | 0              | 0         | 0             | 20     | 0    |
|                 | 1    | 0       | 0    | 0              | 0         | 0             | 0      | 39   |
| Predicted Class |      |         |      |                |           |               |        |      |
| KNN             |      |         |      |                |           |               |        |      |

### KNN

Fig. 9. Confusion matrices for Case3.

Table 8

Accuracy, Precision, Recall, Geometric mean, and F Score results for KNN classification after running 1000 iterations.

| Case   | Statistic          | Accuracy | Precision | Recall | Geometric mean | F-Score |
|--------|--------------------|----------|-----------|--------|----------------|---------|
| Case 1 | Maximum            | 99.45    | 98.78     | 99.52  | 99.52          | 99.15   |
|        | Minimum            | 98.80    | 98.10     | 99.39  | 99.38          | 98.74   |
|        | Mean               | 99.20    | 98.70     | 99.52  | 99.51          | 99.11   |
|        | Standard deviation | 0.09     | 0.20      | 0.014  | 0.015          | 0.11    |
| Case 2 | Maximum            | 99.31    | 99.46     | 99.57  | 99.57          | 99.52   |
|        | Minimum            | 98.50    | 99.24     | 99.39  | 99.39          | 99.32   |
|        | Mean               | 99.00    | 99.45     | 99.56  | 99.56          | 99.51   |
|        | Standard deviation | 0.11     | 0.01      | 0.02   | 0.02           | 0.02    |
| Case 3 | Maximum            | 99.19    | 98.77     | 99.01  | 99.01          | 98.89   |
|        | Minimum            | 98.69    | 97.94     | 98.74  | 98.73          | 98.34   |
|        | Mean               | 98.95    | 98.56     | 98.99  | 98.98          | 98.77   |
|        | Standard deviation | 0.06     | 0.26      | 0.04   | 0.04           | 0.14    |

Decision Tree (DT), Support Vector Machines (SVM), K-Nearest Neighbors (KNN). DT, SVM, and KNN algorithm confusion matrices for Case 1 dataset are shown in Fig. 7, Case 2 dataset confusion matrices in Fig. 8, and Case 3 dataset confusion matrices in Fig. 9.

As seen in Fig. 7, the best results have been calculated with the KNN algorithm. The best result has been calculated in the Bronchiectasis class with the SVM algorithm. In the KNN algorithm, the best result has been computed for the COPD, Bronchiectasis, Pneumonia, and LRTI classes.

As seen in Fig. 8, the best results have been obtained with SVM and KNN algorithms. The best results in both SVM and KNN algorithms have been calculated with the Asthma class.

As seen in Fig. 9, there are eight classes in total. Best results have been calculated by SVM and KNN algorithm. The best result has been computed in the Bronchiectasis class with the SVM algorithm. In the KNN algorithm, the best result has been calculated in Bronchiectasis and Asthma classes.

In the proposed method, Accuracy, Precision, Recall, Geometric mean, and F Score values have been calculated by running 1000 iterations of Case 1, Case 2, and Case 3 datasets with three classification algorithms. Equations 6–10 have been used to calculate Accuracy, Precision, Recall, Geometric mean, and F Score parameters.

$$CACC = \frac{TP_c + TN_c}{TP_c + TN_c + FP_c + FN_c}, c = \{1, 2, \dots, NC\} \quad (6)$$

$$UAR = \frac{1}{NC} \sum_{c=1}^{NC} \frac{TP_c}{TP_c + FN_c} \quad (7)$$

$$UAP = \frac{1}{NC} \sum_{c=1}^{NC} \frac{TP_c}{TP_c + FP_c} \quad (8)$$

$$GM = \sqrt[NC]{\prod_{c=1}^{NC} \frac{TP_c}{TP_c + FN_c}} \quad (9)$$

$$F1 = \frac{2 * (UAP * UAR)}{UAP + UAR} \quad (10)$$

In Eqs. (7)–(10),  $TP_c$  (True Positive Count),  $TN_c$  (True Negative Count),  $FP_c$  (False Positive Count),  $FN_c$  (False Negative Count),  $NC$  (Class Count). The results have been calculated by choosing the recommended method 10 Cross-validation (10 fold crossing). After running 1000 iterations, Accuracy, Precision, Recall, Geometric mean, and F Score parameters have been calculated for KNN classification. The results are shown in Table 8.

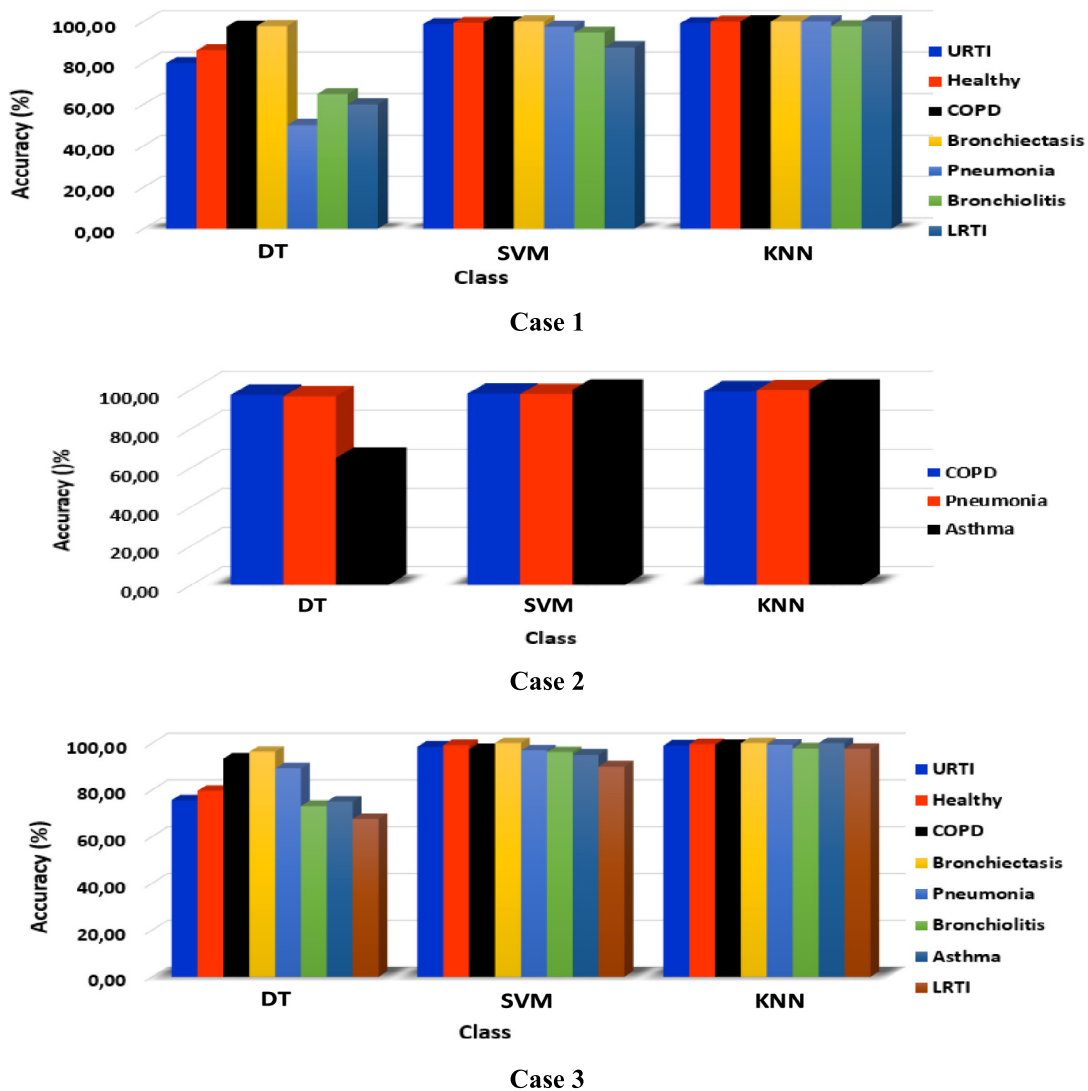


Fig. 10. Class by Class results for Case 1, Case 2, and Case 3.

In the results shown in Table 8, the best result for Case 1 has been calculated with the KNN algorithm. While calculating 83.7% with the DT algorithm and 98.41% with SVM, an accuracy of 99.45% has been calculated with KNN. For Case 2, an accuracy of 96.66%, 97.87%, and 99.31% has been computed using DT, SVM, and KNN algorithms, respectively. Accuracy of 86.41%, 97.8%, and 99.19% has been calculated for Case 3, respectively. The best results for Case 1, Case 2, and Case 3 datasets have been calculated with the KNN algorithm. For the proposed method, Class by Class has been calculated for Case1, Case2, and Case3, and results have been obtained for each class. The Class by Class results obtained are shown in Fig. 10.

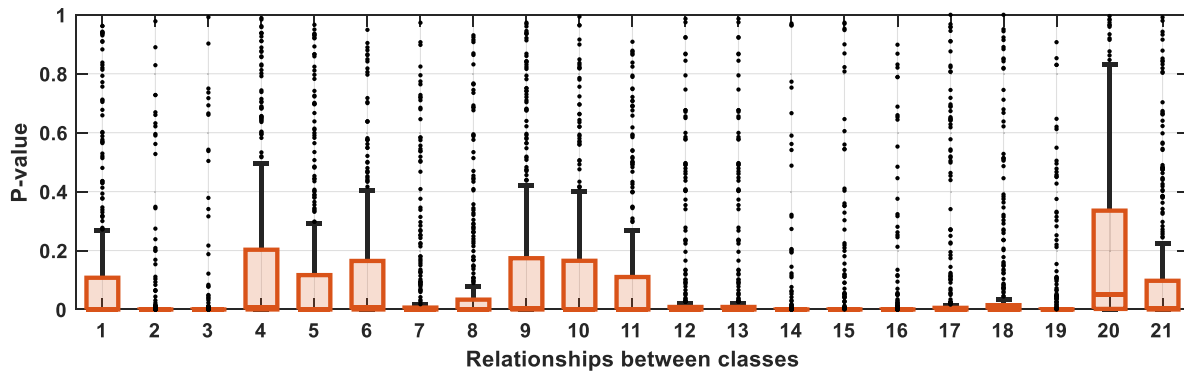
As seen in Fig. 10, SVM and KNN algorithm results have been better than the DT algorithm in Case by Case results for Case1,

Case2, and Case3. The obtained results confirmed the confusion matrix.

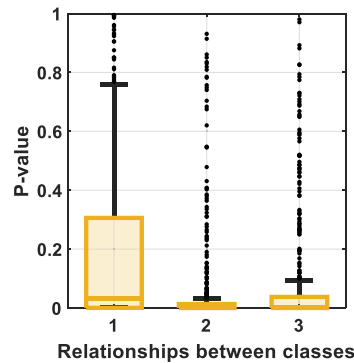
#### 4. Discussion

A hybrid model including TQWT, Piccolo pattern, and statistical methods have been developed for Case1, Case2, and Case3 to achieve high accuracy. For these feature extraction results, the most significant features have been selected using INCA. Thus, 2013x306 for Case1, 1740x463 for Case2, and 3827x451 for Case3 have been selected. The p-value values of the most significant features selected are shown in Fig. 11.

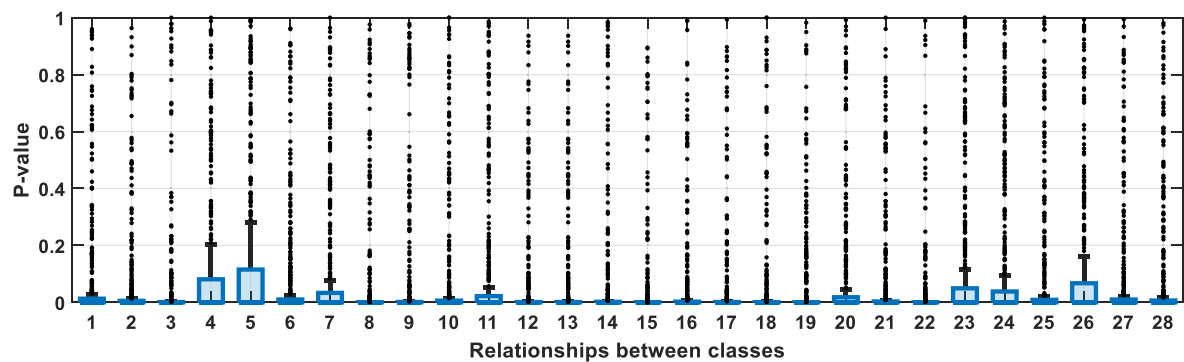
As seen in Fig. 11, a p-value of 21 has been calculated as Case1 had seven classes. Since Case2 had three classes, it had three



Case 1



Case 2



Case 3

Fig. 11. Box plots between classes of features calculated p-value.

**Table 9**  
Performance comparison of lung diseases prediction methods.

| Method                            | Year | Number of classes | Accuracy     | Specialty/Prediction | Sensitivity/Recall | F1 Score |
|-----------------------------------|------|-------------------|--------------|----------------------|--------------------|----------|
| Minami et al. 's method [35]      | 2019 | 4                 | 50           | 69                   | 36                 | –        |
| Ma et al. 's method [49]          | 2019 | 4                 | 52.79        | 69.20                | 31.12              | 50.16    |
| Jaber et al.'s method [14]        | 2020 | 7                 | 98.76        | 99.23                | 98.40              | 98.89    |
| Shuvo et al.'s method [31]        | 2020 | 3                 | 98.9         | 100                  | 98.9               | 99.4     |
|                                   |      | 6                 | 98.7         | 100                  | 98.6               | 99.3     |
| Yang et al. 's method [32]        | 2020 | 4                 | 50.16        | 31.12                | 69.20              | –        |
| Naqvi et al. 's method [33]       | 2020 | 3                 | 97.70        | –                    | –                  | –        |
| Ntalampiras et al. 's method [34] | 2020 | 4                 | 50.1         | –                    | –                  | –        |
| Li et al. 's method [38]          | 2020 | 4                 | 67           | –                    | –                  | –        |
| Demir et al. 's method [39]       | 2020 | 4                 | 71.15        | 86                   | 61                 | 65       |
| Pham et al. 's method [40]        | 2020 | 4                 | 79           | 90                   | 68                 | –        |
|                                   |      | 2                 | 84           | 90                   | 78                 | –        |
| Demir et al. 's method [41]       | 2020 | 4                 | 65.5         | 83                   | 53                 | 55       |
| Ngo et al. 's method [43]         | 2020 | 4                 | 49           | 69                   | 30                 | –        |
| Acharya et al. 's method [44]     | 2020 | 4                 | 71.81        | 86.70                | 56.91              | –        |
| Hazra et al. 's method [45]       | 2020 | 6                 | 92           | 71.83                | 50.83              | 54.83    |
| Pham et al. 's method [46,47]     | 2020 | 4                 | 86           | 88                   | 85                 | –        |
| Nguyen et al. 's method [48]      | 2020 | 4                 | 78.4         | 87.3                 | 69.4               | –        |
|                                   |      | 2                 | 83.7         | 87.3                 | 80.01              | –        |
| Monaco et al. 's method [51]      | 2020 | 2                 | 82           | 87                   | –                  | –        |
| Fraïwan et al. 's method [36]     | 2021 | 6                 | 98.27        | –                    | –                  | 93.61    |
| Mukherjee et al. 's method [37]   | 2021 | 2                 | 99.22        | –                    | –                  | –        |
| Our method – Case 1 – DT          | –    | 7                 | 83.70        | 78.91                | 77.76              | 78.33    |
| Our method – Case 1 – SVM         |      |                   | 98.41        | 99.01                | 96.97              | 97.86    |
| Our method – Case 1 – KNN         |      |                   | <b>99.45</b> | 98.78                | 99.52              | 99.15    |
| Our method – Case 2 – DT          |      | 3                 | 96.66        | 97.19                | 94.35              | 94.37    |
| Our method – Case 2 – SVM         |      |                   | 97.87        | 98.48                | 98.55              | 98.51    |
| Our method – Case 2 – KNN         |      |                   | <b>99.31</b> | 99.46                | 99.57              | 99.52    |
| Our method – Case 3 – DT          |      | 8                 | 86.41        | 82.40                | 82.06              | 81.59    |
| Our method – Case 3 – SVM         |      |                   | 97.80        | 98.19                | 96.63              | 97.40    |
| Our method – Case 3 – KNN         |      |                   | <b>99.19</b> | 98.77                | 99.01              | 98.89    |

\*The highest value for each metric is shown in bold.

p-value values, and Case3 had eight classes; therefore, 28p-value values have been computed.

There are many studies in the literature using ICBHI 17 dataset. The proposed method and the results in the literature are compared in Table 9.

As seen in Table 9, performance results for two, three, four, and six classes have been calculated by using ICBHI 17 dataset in the literature. In the proposed method, performance results have been computed for three, seven, and eight classes. Case1, Case2, and Case3 have been created to calculate these classes. In the literature, the best accuracy for three classes has been calculated to be 98.9% [31]. Shuvo et al. [31] proposed the Lightweight CNN model in their study and used healthy, chronic, and non-chronic classes. The Naqvi et al. [33] study calculated accuracy of 97.70% for three classes. Naqvi used the ICBHI dataset obtained from Meditron Littmann 3200 and Littmann Classic instruments. It used DT, LD, and SVM algorithms for the classification step. In this study, 99% accuracy has been calculated for three classes in Case2. The best result has been obtained with the KNN algorithm. Many deep learning methods using four and six classes in the ICBHI dataset have been proposed in the literature[40,45]. The best accuracy value using four classes in the ICBHI dataset was calculated by Pham et al. [46,47], who calculated 86% accuracy for normal, crackle, wheeze, both classes. Shuvo et al. [31] calculated 98.9% accuracy for both three classes and six classes in the same study. Jaber et al. [14] calculated the best accuracy (98.76%) for seven classes in the literature. In the present study, an accuracy of 99.45% has been computed for seven classes. In the literature, eight-class results have not been calculated using the ICBHI 17 dataset. In the proposed method, an accuracy rate of 99.19% has been calculated for the eight classes. Case1, Case2, and Case3 have been created in this study, and the results have been calculated using DT, SVM, and KNN algorithms. Contribution to the literature is provided by calculating the highest accuracy values for three, seven, and eight

classes. A hybrid model based on TQWT, Piccolo pattern, and statistical has been developed for feature extraction in this study.

## 5. Conclusions

To summarize, this study has been conducted using the ICBHI Challenge database, which contains 928 sound recording data collected and labeled with eight types of lung disease from 126 individuals with an electronic stethoscope. In the study, a method has been developed for lung disease detection problems with eight classes, seven classes, and three classes for three different test sets. This method's basic steps were: feature generation using the proposed Piccolo pattern and statistical methods, the most informative feature selection using INCA, and classification with three shallow classifiers. The present study results revealed that this method achieved a classification accuracy of 99.45%, 99.31%, and 99.19% for Case 1: seven-class, Case 2: three-class, and Case 3: eight-class problem using the KNN classifier (see Table 9). These results demonstrated the success of the nonlinear model-based lung disease classification method.

## 6. Future works

The architecture of the application planned in future studies according to the experimental results is shown below. In this study, a lightweight method has been proposed for the detection and classification of pulmonary diseases. The proposed method has been more successful than the deep learning studies in the literature. A TQWT, Piccolo pattern and statistical-based hybrid model has been developed in the proposed method, and high accuracy has been calculated. In this sense, it can be argued that the proposed hybrid model has made significant contributions to the field. Traditional methods have been used for classification. Traditional methods do not require high servers, such as deep learning.



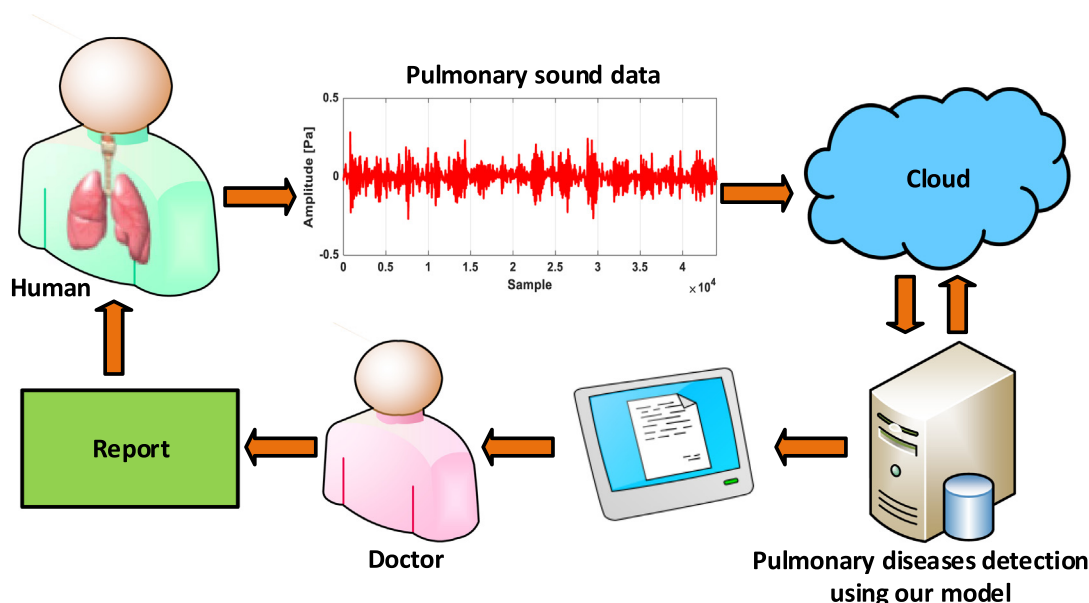


Fig. 12. The architecture of the planned cloud-based automated pulmonary diseases detection application.

Thus, the application cost has been low. In addition, the proposed method below has high real-time operability. In the future, a real-time application that can be used in smart hospitals is planned. The stages of our intended smart monitoring and detection model are shown in Fig. 12. First of all, the lung sounds of the patient will be collected at the early diagnosis stage. The sounds obtained will be transferred to the presentation via the cloud. The model will develop on the server works. The obtained reports will be forwarded to the doctor. Intelligent assistants will be developed in the medical field. Thus, doctors will be able to treat more patients. The proposed model will contribute to early and accurate diagnosis processes.

#### CRediT authorship contribution statement

**Beyda Tasar:** Conceptualization, Validation, Resources, Writing – original draft, Writing – review & editing, Visualization. **Orhan Yaman:** Validation, Investigation, Data curation, Writing – review & editing, Visualization, Methodology, Software. **Turker Tuncer:** Writing – review & editing, Visualization, Methodology.

#### Declaration of Competing Interest

The authors declare that they have no known competing financial interests or personal relationships that could have appeared to influence the work reported in this paper.

#### References

- [1] Forum of International Respiratory Societies. The Global Impact of Respiratory Disease. 2017.
- [2] Kassebaum NJ, Arora M, Barber RM, Brown J, Carter A, Casey DC, et al. Global, regional, and national disability-adjusted life-years (DALYs) for 315 diseases and injuries and healthy life expectancy (HALE), 1990–2015: a systematic analysis for the Global Burden of Disease Study 2015. *Lancet* 2016;388:1603–58. [https://doi.org/10.1016/S0140-6736\(16\)31460-X](https://doi.org/10.1016/S0140-6736(16)31460-X).
- [3] Diseases CR. Chronic Respiratory n.d.:12–36.
- [4] Burney PGJ, Patel J, Newson R, Minelli C, Naghavi M. Global and regional trends in COPD mortality, 1990–2010. *Eur Respir J* 2015;45:1239–47. <https://doi.org/10.1183/09031936.00142414>.
- [5] Network GA. The Global Asthma Report 2014. 2014.
- [6] Pearce N, Ait-Khaled N, Beasley R, Mallol J, Keil U, Mitchell EA, et al. Worldwide trends in the prevalence of asthma symptoms: Phase III of the International Study of Asthma and Allergies in Childhood (ISAAC). *Thorax* 2007;62:757–65. <https://doi.org/10.1136/thx.2006.070169>.
- [7] World Health Organization. Influenza (Seasonal) Ask the expert : Influenza Q & A. Who 2018;2020:1–5.
- [8] World Health Organization. Global Tuberculosis Report. 2021.
- [9] Sung H, Ferlay J, Siegel RL, Laversanne M, Soerjomataram I, Jemal A, et al. Global Cancer Statistics 2020: GLOBOCAN Estimates of Incidence and Mortality Worldwide for 36 Cancers in 185 Countries. *CA Cancer J Clin* 2021;71:209–49. <https://doi.org/10.3322/caac.21660>.
- [10] Rocha BM, Filos D, Mendes L, Serbes G, Ulukaya S, Kahya YP, et al. An open access database for the evaluation of respiratory sound classification algorithms. *Physiol Meas* 2019;40. <https://doi.org/10.1088/1361-6579/ab03ea>.
- [11] Sovijärvi ARA, Vanderschoot J, Earis JE. Standardization of computerized respiratory sound analysis. *Eur Respir Rev* 2000;10:585.
- [12] Rocha BM, Filos D, Mendes L, Vogiatzis I, Perantoni E, Kaimakamis E, et al. A Respiratory Sound Database for the Development of Automated Classification. Springer 2017.
- [13] Pramono RXA, Bowyer S, Rodriguez-Villegas E. Automatic adventitious respiratory sound analysis: A systematic review. vol. 12. 2017. 10.1371/journal.pone.0177926.
- [14] Jaber MM, Abd SK, Shakeel PM, Burhanuddin MA, Mohammed MA, Yusoff S. A telemedicine tool framework for lung sounds classification using ensemble classifier algorithms. *Meas J Int Meas Confed* 2020;162:. <https://doi.org/10.1016/j.measurement.2020.107883>.
- [15] Ojala T, Pietikainen M, Harwood D. Performance evaluation of texture measures with classification based on Kullback discrimination of distributions. *Proc. 12th Int. Conf. Pattern Recognit.* 1994;1:582–5.
- [16] Dokur Z. Respiratory sound classification by using an incremental supervised neural network. *Pattern Anal Appl* 2009;12:309–19. <https://doi.org/10.1007/s10044-008-0125-y>.
- [17] Sarkar M, Madabhavi I, Niranjan N, Dogra M. Auscultation of the respiratory system. *Ann Thorac Med* 2015;10:158–68. <https://doi.org/10.4103/1817-1737.160831>.
- [18] Arts L, Lim EHT, van de Ven PM, Heunks L, Tuinman PR. The diagnostic accuracy of lung auscultation in adult patients with acute pulmonary pathologies: a meta-analysis. *Sci Rep* 2020;10:1–11. <https://doi.org/10.1038/s41598-020-64405-6>.
- [19] Fukumitsu T, Obase Y, Ishimatsu Y, Nakashima S, Ishimoto H, Sakamoto N, et al. The acoustic characteristics of fine crackles predict honeycombing on high-resolution computed tomography. *BMC Pulm Med* 2019;19:1–7. <https://doi.org/10.1186/s12890-019-0916-5>.
- [20] Bohadana A, Izbicki G, Kraman SS. Fundamentals of Lung Auscultation. *N Engl J Med* 2014;370:744–51. <https://doi.org/10.1056/nejmra1302901>.
- [21] Vyshebskiy A, Alhashem RM, Paciej R, Ebril M, Rudman I, Fredberg JJ, et al. Mechanism of inspiratory and expiratory crackles. *Chest* 2009;135:156–64. <https://doi.org/10.1378/chest.07-1562>.
- [22] García-Ordás MT, Benítez-Andrades JA, García-Rodríguez I, Benavides C, Alaiz-Moretón H. Detecting respiratory pathologies using convolutional neural networks and variational autoencoders for unbalancing data. *Sensors (Switzerland)* 2020;20. 10.3390/s20041214.
- [23] Kim Y, Hyon YK, Jung SS, Lee S, Yoo G, Chung C, et al. Respiratory sound classification for crackles, wheezes, and rhonchi in the clinical field using deep learning. *Sci Rep* 2021;11:1–11. <https://doi.org/10.1038/s41598-021-96724-7>.

- [24] Roguin A. Rene theophile hyacinthe laënnec (1781–1826): The man behind the stethoscope. *Clin Med Res* 2006;4:230–5. <https://doi.org/10.3121/cmr.4.3.230>.
- [25] Suppakitjanusant P, Sungkanuparph S, Wongsinin T, Virapongsiri S, Kasemkosin N, Chailurkit L, et al. Identifying individuals with recent COVID-19 through voice classification using deep learning. *Sci Rep* 2021;11:1–7. <https://doi.org/10.1038/s41598-021-98742-x>.
- [26] Mohammed EA, Keyhani M, Sanati-Nezhad A, Hejazi SH, Far BH. An ensemble learning approach to digital corona virus preliminary screening from cough sounds. *Sci Rep* 2021;11:1–11. <https://doi.org/10.1038/s41598-021-95042-2>.
- [27] Siontis KC, Noseworthy PA, Attia ZI, Friedman PA. Artificial intelligence-enhanced electrocardiography in cardiovascular disease management. *Nat Rev Cardiol* 2021;18:465–78. <https://doi.org/10.1038/s41569-020-00503-2>.
- [28] Aydemir E, Tuncer T, Dogan S. A Tunable-Q wavelet transform and quadruple symmetric pattern based EEG signal classification method. *Med Hypotheses* 2020;134:. <https://doi.org/10.1016/j.mehy.2019.109519>109519.
- [29] Shibutani K, Isobe T, Hiwatari H, Mitsuda A, Akishita T, Shirai T. Piccolo: An ultra-lightweight blockcipher. *Lect Notes Comput Sci (Including Subser Lect Notes Artif Intell Lect Notes Bioinformatics)* 2011;6917 LNCS:342–57. 10.1007/978-3-642-23951-9\_23.
- [30] Tuncer T, Dogan S, Ertam F. Automatic voice based disease detection method using one dimensional local binary pattern feature extraction network. *Appl Acoust* 2019;155:500–6. <https://doi.org/10.1016/j.apacoust.2019.05.023>.
- [31] Shuvo SB, Ali SN, Swapnil SI, Hasan T, Bhuiyan MH. A lightweight CNN model for detecting respiratory diseases from lung auscultation sounds using EMD-CWT-based hybrid scalogram. *ArXiv* 2020;XX:1–9. <https://doi.org/10.1109/ibhi.2020.3048006>.
- [32] Yang Z, Liu S, Song M, Parada-Cabaleiro E, Schuller BW. Adventitious respiratory classification using attentive residual neural networks. *Proc Annu Conf Int Speech Commun Assoc INTERSPEECH* 2020;2020-Octob:2912–6. 10.21437/Interspeech.2020-2790.
- [33] Nalampi S, Potamitis I. Automatic acoustic identification of respiratory diseases. *Evol Syst* 2020. <https://doi.org/10.1007/s12530-020-09339-0>.
- [34] Minami K, Lu H, Kim H, Mabu S, Hirano Y, Kido S. Automatic Classification of Large-Scale Respiratory Sound Dataset Based on Convolutional Neural Network. *Int Conf Control Autom Syst* 2019;2019-Octob:804–7. 10.23919/ICCAS47443.2019.8971689.
- [35] Fraiwan L, Hassani O, Fraiwan M, Khassawneh B, Ibnian AM, Alkhodari M. Automatic identification of respiratory diseases from stethoscopic lung sound signals using ensemble classifiers. *Biocybern Biomed Eng* 2021;41:1–14. <https://doi.org/10.1016/j.bbe.2020.11.003>.
- [36] Mukherjee H, Sreerama P, Dhar A, Obaidullah SM, Roy K, Mahmud M, et al. Automatic Lung Health Screening Using Respiratory Sounds. *J Med Syst* 2021;45. <https://doi.org/10.1007/s10916-020-01681-9>.
- [37] Li C, Du H, Zhu B. Classification of Lung Sounds Using Classification of lung sounds using CNN-. *Attention* 2020.
- [38] Demir F, Ismael AM, Sengur A. Classification of Lung Sounds with CNN Model Using Parallel Pooling Structure. *IEEE Access* 2020;8:105376–83. <https://doi.org/10.1109/ACCESS.2020.3000111>.
- [39] Pham L, Phan H, Palaniappan R, Mertins A, McLoughlin I. CNN-MoE based framework for classification of respiratory anomalies and lung disease detection. *ArXiv* 2020.
- [40] Demir F, Sengur A, Bajaj V. Convolutional neural networks based efficient approach for classification of lung diseases. *Heal Inf Sci Syst* 2020;8:1–8. <https://doi.org/10.1007/s13755-019-0091-3>.
- [41] Thi T, Nguyen K, Pernkopf F. Crackle Detection in Lung Sounds Using Transfer Learning and Multi-Input Convolutional Neural Networks Multi-Input Convolutional Neural Networks 2020.
- [42] Ngo D, Pham L, Nguyen A, Phan B, Tran K, Nguyen T. Deep Learning Framework Applied for Predicting Anomaly of Respiratory Sounds 2020.
- [43] Acharya J, Basu A. Deep Neural Network for Respiratory Sound Classification in Wearable Devices Enabled by Patient Specific Model Tuning. *ArXiv* 2020;14:535–44.
- [44] Hazra R, Majhi S. Detecting respiratory diseases from recorded lung sounds by 2D CNN. In: *Proc 2020 Int Conf Comput Commun Secur ICCCS*. <https://doi.org/10.1109/ICCCS49678.2020.9277101>.
- [45] Pham L, Phan H, King R, Mertins A, McLoughlin I. Inception-Based Network and Multi-Spectrogram Ensemble Applied For Predicting Respiratory Anomalies and Lung Diseases 2020:18–21.
- [46] Pham L, McLoughlin I, Phan H, Tran M, Nguyen T, Palaniappan R. Robust deep learning framework for predicting respiratory anomalies and diseases. *ArXiv* 2020;5–8.
- [47] Nguyen T, Pernkopf F. Lung Sound Classification Using Snapshot Ensemble of Convolutional Neural Networks. *Proc Annu Int Conf IEEE Eng Med Biol Soc EMBS* 2020;2020-July:760–3. 10.1109/EMBC44109.2020.9176076.
- [48] Ma Y, Xu X, Yu Q, Zhang Y, Li Y, Zhao J, et al. Lungbrn: A smart digital stethoscope for detecting respiratory disease using bi-resnet deep learning algorithm. *BioCAS 2019 - Biomed Circuits Syst Conf Proc* 2019:1–4. 10.1109/BIOCAS.2019.8919021.
- [49] Paraschiv E-A, Rotaru C-M. Machine Learning Approaches based on Wearable Devices for Respiratory Diseases Diagnosis 2020:1–4. 10.1109/ehb50910.2020.9280098.
- [50] Monaco A, Amoroso N, Bellantuono L, Pantaleo E, Tangaro S, Bellotti R. Multi-time-scale features for accurate respiratory sound classification. *Appl Sci* 2020;10:1–17. <https://doi.org/10.3390/app10238606>.
- [51] Basu V, Rana S. Respiratory diseases recognition through respiratory sound with the help of deep neural network. *4th Int Conf Comput Intell Networks, CINE* 2020 2020. 10.1109/CINE48825.2020.234388.
- [52] Gairola S, Tom F, Kwatra N, Respirenet JM. A deep neural network for accurately detecting abnormal lung sounds in limited data setting. *ArXiv* 2020:1–7.
- [53] Ding J, Zhou J, Yin Y. Fault detection and diagnosis of a wheelset-bearing system using a multi-Q-factor and multi-level tunable Q-factor wavelet transform. *Meas J Int Meas Confed* 2019;143:112–24. <https://doi.org/10.1016/j.measurement.2019.05.006>.
- [54] Khare SK, Bajaj V. Constrained based tunable Q wavelet transform for efficient decomposition of EEG signals. *Appl Acoust* 2020;163:. <https://doi.org/10.1016/j.apacoust.2020.107234>107234.
- [55] Tuncer T, Ertam F. Neighborhood component analysis and reliefF based survival recognition methods for Hepatocellular carcinoma. *Phys A Stat Mech Its Appl* 2020;540:. <https://doi.org/10.1016/j.physa.2019.123143>123143.
- [56] Tuncer T, Ozyurt F, Dogan S, Subasi A. A novel Covid-19 and pneumonia classification method based on F-transform. *Chemom Intell Lab Syst* 2021;210:. <https://doi.org/10.1016/j.chemolab.2021.104256>104256.